Photocurable Epoxy/Cubic Silsesquioxane Hybrid Materials for Polythiourethane: Failure Mechanism of Adhesion under Weathering

Khine Yi Mya,[1] Norio Nakayama,[2] Toshihiko Takaki,[2] Yang Xiao,[1] Ting Ting Lin,[1] Chaobin He[1]

[1]*Institute of Materials Research and Engineering, 3-Research Link, Singapore 117602*
[2]*Mitsui Chemicals Inc., 580-32, Nagaura, Sodegaura-Shi, Chiba 2990265, Japan*

Received 4 July 2007; accepted 17 August 2007
DOI 10.1002/app.27640
Published online 27 December 2007 in Wiley InterScience (www.interscience.wiley.com).

ABSTRACT: A new inorganic–organic hybrid coating containing epoxy-functionalized cubic silsesquioxane (CSSQ) has been developed, which can be polymerized cationically by UV radiation. This solvent-free solution can be used as hybrid coating for polythiourethane (PTU) substrate. The surface properties of the coating film were determined by adhesion and scratch resistance. The excellent adhesion of coating films on the substrate was observed at the initial stage before weathering, but deteriorated after exposure to the sunshine. The low viscosity of hybrid coating solution (~ 15 mPa s) leads to fast curing and the formation of hybrid coating film during the photopolymerization reaction. The adhesion failure was evaluated by atomic force microscopy (AFM), Fourier transform infrared spectroscopy (FTIR), and X-ray photoelectron spectroscopy (XPS) analyses. AFM images showed that the surface is smooth at the initial stage, but a texture surface was developed after weathering. The shrinkage of the hybrid film due to the increase in crosslinking density by postpolymerization would affect the surface roughness after weathering. XPS analysis indicated that the adhesion failure occurred by photodegradation of the PTU substrate during weathering. The weathering resistance was significantly improved by adding UV absorbers, which protected the polymer substrate from the photodegradation. The advantages of the hybrid coating include fast cure speed, solvent-free formulation, and improved surface properties of the coating film. © 2007 Wiley Periodicals, Inc. J Appl Polym Sci 108: 181–188, 2008

Key words: adhesion; cubic silsesquioxane; photopolymerization; coatings; failure

INTRODUCTION

Cationic photopolymerization ultraviolet (UV) curable coatings have received considerable attention in many industrial applications such as plastics, electronics, protective coatings, and adhesives due to their rapid and solvent-free curing of coating films.[1,2] There has been growing interest in solvent-free UV curing systems because of environmental concerns. Most of the applications of UV curing are found in the coating industry for the surface protection of various materials by fast-drying varnishes, paints, or printing inks.[3] Cationic photoinduced polymerization process could offer some benefits compared to the radical photopolymerization, in particular relatively low shrinkage during curing, no oxygen inhibition, good adhesion to the substrate, and high chemical resistance.[2,4–6] However, an investigation of the photoinitiated cationic ring-opening polymerization of epoxy monomers showed that certain monomers displayed low reactivity in photoinduced cationic polymerization, which are not suitable for commercial applications.[7,8] Crivello and Mao[9] introduced the photoinduced cationic polymerization of multifunctional siloxane oligomers. These oligomers exhibited extremely rapid photoinduced cationic polymerization and high conversion rate even in the case of multifunctional oligomers. The rapid curing and the resulting excellent physical properties lead to many applications of these materials such as dental restorative materials and coatings for optoelectronic devices.[10–12]

Recently, inorganic–organic hybrid coatings are widely used as interfacial modifiers to improve the properties such as adhesion, barrier properties, and mechanical strength.[4,13–17] Cubic silsesquioxanes (CSSQ) possess unique characteristics with a well-defined, three-dimensional nanostructure containing silica cage and the organic functional groups on the silica cage surface with a diameter range of 0.5–1.5 nm.[18–21] It has been found to offer attractive properties that include improved thermal stability, chemical resistance, and enhancements in mechanical properties.[22–25] For example, methacrylate-functionalized CSSQ-based dental restorative composites,

Correspondence to: C. He (cb-he@imre.a-star.edu.sg).
Contract grant sponsor: Institute of Materials, Research and Engineering (under the Agency for Science, Technology, and Research (A*STAR), Singapore).

Journal of Applied Polymer Science, Vol. 108, 181–188 (2008)

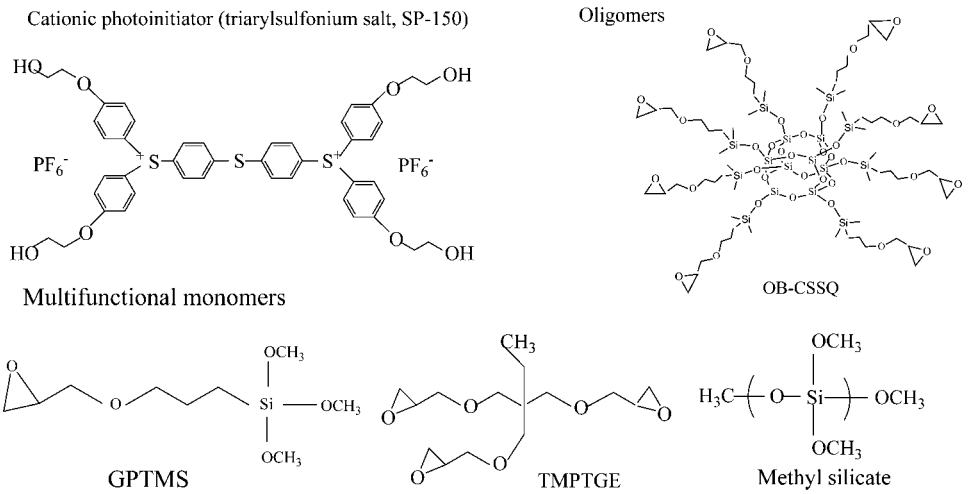

Figure 1 The chemical structures of UV hybrid coating composition.

prepared via photoinitiated free radical polymerization, are found to improve mechanical strength.[26] Su et al.[17] reported that thermal mechanical properties of acrylic polymers were subsequently enhanced by incorporating nanosized polysilsesquioxane. In the present work, multifunctional epoxy monomers and oligomers including epoxy-functionalized CSSQ were polymerized cationically by UV radiation in the presence of cationic photoinitiator, particularly, for application in lenses. There has been a high demand for lenses having light weight and high refractive index, polythiourethane (PTU) with refractive index of 1.60–1.67 was used as a polymer substrate in this report.

Organic coating materials are known to undergo degradation when exposed to UV radiation, leading to discoloration, cracking, and embrittlement upon weathering.[27] Although a few studies[27–29] reported the remarkable performance of UV-curable coating, the potential of these systems for increasing the weather resistance of polymer coatings has not been achieved.

In this study, new photocurable epoxy/cubic silsesquioxane hybrid materials are reported. The hybrid materials using the cationic photopolymerization UV-curable resin containing epoxy-functionalized CSSQ were prepared, and the failure mechanism of the hybrid films were evaluated by atomic force microscopy (AFM), Fourier transform infrared spectroscopy (FTIR), and X-ray photoelectron spectroscopy (XPS) studies.

EXPERIMENTAL

Materials

3-Glycidyloxypropyltrimethoxy silane (GPTMS, 98%) was purchased from Aldrich, and trimethylolpropane triglycidyl ether (Epolite 100MF, TMPTGE) was obtained from Kyoeisha Co., Japan. Bis[4-(di(4-(2-hydroxyethyl)phenyl)sulfonio-phenyl] sulfide bis-hexafluorophosphate (SP-150) from Asahi Denka Co. was used as a cationic photoinitiator. Methyl silicate-51 (Tama Chemicals Co.) was applied to develop silica networks because it acts as a four functional building block. 2,2′,4,4′-tetrahydroxybenzophenone (THBP), hydroxyphenyltriazine (HPT), and benzotriazole (BTZ) from Ciba Specialty Chemicals were used as ultraviolet (UV) absorbers in some cases. Octakis(dimethylsiloxy)octasilsesquioxane ($Q_8M_8^H$) was purchased from Hybrid Plastics, and allyl glycidyl ether (AGE, ≥99%) was obtained from Aldrich. Octa[2-(butoxymethyl)oxirane di-methylsiloxy] silsesquioxane, namely, OB-CSSQ (epoxy-functionalized CSSQ) was prepared in our laboratory according to the literature.[30] The viscosity of OB-CSSQ was found to be ~ 300 mPa s. All the chemical structures are shown in Figure 1.

Preparation of oligomer GPTMS (O-GPTMS)

A partial condensate of 3-glycidyloxypropyltrimethoxy silane (O-GPTMS) was prepared by the method reported by Crivello and Mao[9] with slight modification. In a typical procedure, 1% solution of hydrochloric acid (HCl, 0.5 mL) was added into a mixture of 236 g (1 mol) of GPTMS and 27 g (15 mol) of deionized water and stirred at room temperature for

TABLE I
The Relative Intensity Ratio of T_0–T_3

T_0 (−43 ppm)	T_1 (−50 ppm)	T_2 (−58 ppm)	T_3 (−66 ppm)
29.2	17.6	36.5	16.7

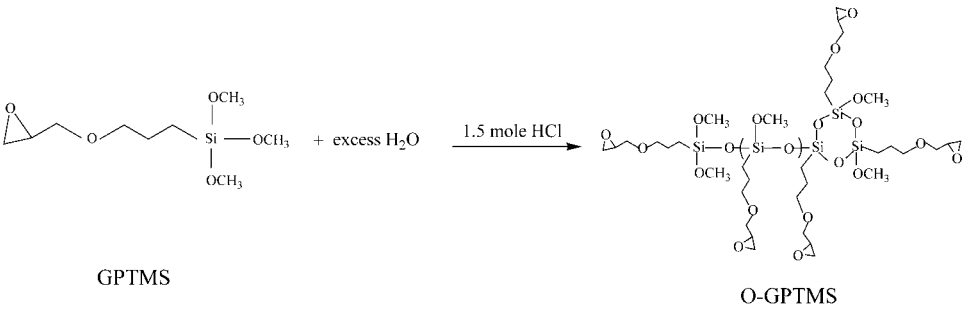

Figure 2 The synthetic procedure of O-GPTMS.

24 h. Anhydrous toluene (100 g) was then added to the mixture. A partial condensate of clear, viscous oligomer (O-GPTMS) was obtained after the removal of toluene and water, and the product was characterized by ^{29}Si-NMR. The degree of condensation was calculated by integration of the individual signals from ^{29}Si-NMR according to the following equation;

$$K(\%) = \frac{T_1 + 2T_2 + 3T_3}{3(T_0 + T_1 + T_2 + T_3)} \quad (1)$$

where K is the condensation grade and T_x is the number of siloxane groups bound to the Si-atom. The relative intensity ratio of T_0 to T_3 was displayed in Table I and the degree of condensation was found to be $\sim$ 47% (Fig. 2).

Methodology

The viscosity of the hybrid compositions listed in Table II was measured by Brookfield cone and plate viscometer (model: LV-RV-HA-HB-DV-E, Toki Sangyo Co., Japan) at 25°C. The liquid coating formulations were applied to polythiourethane (PTU) substrate by spin-coating (1000 rpm for 10–30 s), and the wet films were exposed to UV radiation (light intensity 150 mW/cm^2; wavelength 365 nm) with high-pressure mercury lamp for 20 s using a conveyor-type UV reactor. The extent of polymerization was determined by FTIR spectroscopy, monitoring the decrease in epoxy absorption band at 844 cm^{-1} upon UV radiation. The thickness of the hybrid film was $\sim$ 5 μm, measured by a stylus-type surface profiler (Veeco Instruments).

The photopolymerization rate was measured using a Q100 differential scanning calorimeter (DSC) (TA Instruments) equipped with a photocalorimeter (PCA). All measurements were carried out at 30°C, and the light intensity was kept at 150 mW/cm^2 under N_2. About 7 mg homogeneous solution was weighed into the aluminum pan, which controlled the sample weight for each test. The data were analyzed using the TA Instruments Universal Analysis software.

Weather resistance (weathering) test was carried out in the presence of water and a pseudoexposure light using a sunshine weather meter with carbon-arc lamp (Suga Test Instruments Co., Japan). Adhesion of the hybrid films before and after weathering was tested by crosscut peeling test according to Japanese Industrial Standard (JIS-K5600). In a typical procedure, 25 meshes of 1 mm^2 were formed by inserting cut lines on the samples at an interval of 1 mm using an equal-interval spacer and a cutter knife. A transparent, low-pressure adhesive tape was then attached on the samples and peeled by pulling at an angle of 60°, and the meshes remaining on the hybrid film were evaluated by rank 0 (0/100; no adhesion) to rank 7 (100/100; excellent adhesion). In rank 7, the edges of cuts are complete and smooth so that there is no peeled-off grid meshes. The transparency of the film was determined by film transmittance meter (Shimadzu UV 2200). The adhesion failure mechanisms of the UV-cured films were evaluated by atomic force microscopy (AFM) (Surface Science Instrument, model: SSX-100), Fourier transform infrared spectroscopy (FTIR) (Perkin Elmer Instrument, 2000 FTIR spectrometer), and X-ray photoelectron spectroscopy (XPS) (Seiko Instruments, model; nanopics 1000) studies.

RESULTS AND DISCUSSION

The UV-curable coating composition consisted of three main components: (1) mono/multifunctional monomers, (2) functionalized oligomers, and (3)

TABLE II
The Composition Ratios of Hybrid Coating Formulation

Ingredients	Composition ratios (wt %)
GPTMS	48
O-GPTMS	9
OB-CSSQ	17
TMPTGE	13
Methyl silicate	9
Photoinitiator (SP-150)	4

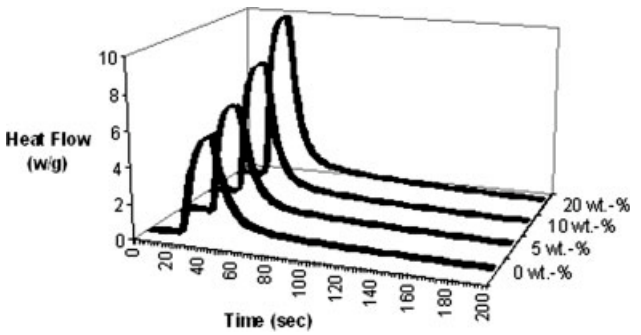

Figure 3 Rate of photopolymerization as a function of irradiation time at various contents of OB-CSSQ.

cationic photoinitiator. The viscosity of the coating solution (formulation is shown in Table II) was found to be ~ 15 mPa s. Because of the low viscosity of hybrid coating solution, the active species gain sufficient mobility to react with the epoxy groups, which leads to fast curing and the formation of hybrid coating film during the photopolymerization reaction. By viewing with naked eyes, no tackiness and defects in coating films such as discontinuities, nonsmoothness, or generation of a texture were observed. The hybrid film showed highly transparent to visible light (>90% transmittance at 400–600 nm wavelength) and improved hardness and scratch resistance in the presence of epoxy-functionalized CSSQ. The structure of OB-CSSQ consists of eight flexible long chains with epoxy end groups, which are favorable to incorporate with hardener in some extents and leads to the high crosslink density.[31] As a result, the incorporation of nanosized epoxy-functionalized CSSQ improves the network formation of the resulting film and increases the rigidity of the nanocomposite films.

Kinetics of photopolymerization

Figure 3 shows the measured heat flow versus irradiation time at various amount of OB-CSSQ. It shows that how OB-CSSQ affects the rate of polymerization. As shown in Figure 3, the time to reach the equilibrium exotherm peak slightly reduced by adding OB-CSSQ (40 s at 0 wt %, 36 sec at 5 wt %, 34 s at 10 wt %, and 32 s at 20 wt %, respectively). The maximum heat flow also increased with increasing amount of OB-CSSQ. It is clear that not only the large epoxy groups in OB-CSSQ induced the rate of polymerization but also due to the decrease in viscosity of the coating solution in the addition of OB-CSSQ. The decrease in viscosity with increasing amount of OB-CSSQ has been reported in our previous article.[31] The increasing number of epoxy groups in OB-CSSQ proceeds the exothermic nature of ring-opening polymerization, which leads the polymerization to higher conversion. The coating formulation for the kinetic study is shown in Table III. The results indicate that the reactivity is higher in the presence of OB-CSSQ.

Weathering of UV-cured hybrid coating

The weathering stability of the coated substrate was first studied. Figure 4 shows the optical micrographs (OM) and topographical AFM images (3.5 μm × 3.5 μm) of the hybrid coating surface before and after exposing to carbon-arc lamp using sunshine weather meter. The optical micrographs were captured using high-resolution digital video microscope (VH-6300) equipped with high-range zoom lens (VH-Z450). The excellent adhesion of hybrid films on PTU substrate was observed at the initial stage before weathering, but it seems deteriorated after weathering at long exposure time. Study showed that the adhesion (peel-off strength) of hybrid coating decreased from rank 7 to rank 1 as shown in Figure 4(a).

AFM was used to understand the failure mechanism of hybrid coating under weathering, and the AFM micrographs are shown in Figure 4(b). At the initial stage before weathering, the surface is smooth but a rough (texture) surface was developed after weathering. The roughness of the hybrid films (R_a) coated on the PTU substrates changed from 0.44 nm before weathering to 0.79 nm after weathering as evaluated from AFM images.

It was mentioned that the cationic photoinitiators are able to form Bronsted acid for the cationic initiation

TABLE III
The Chemical Composition of the Coating Solution with Different OB-CSSQ Content for the Kinetic Study

Ingredients	Composition 1 (wt %)	Composition 2 (wt %)	Composition 3 (wt %)	Composition 4 (wt %)
GPTMS	65	60	55	45
OB-CSSQ	0	5	10	20
O-GPTMS	9	9	9	9
TMPTGE	13	13	13	13
Methyl silicate	9	9	9	9
Photoinitiator (SP-150)	4	4	4	4

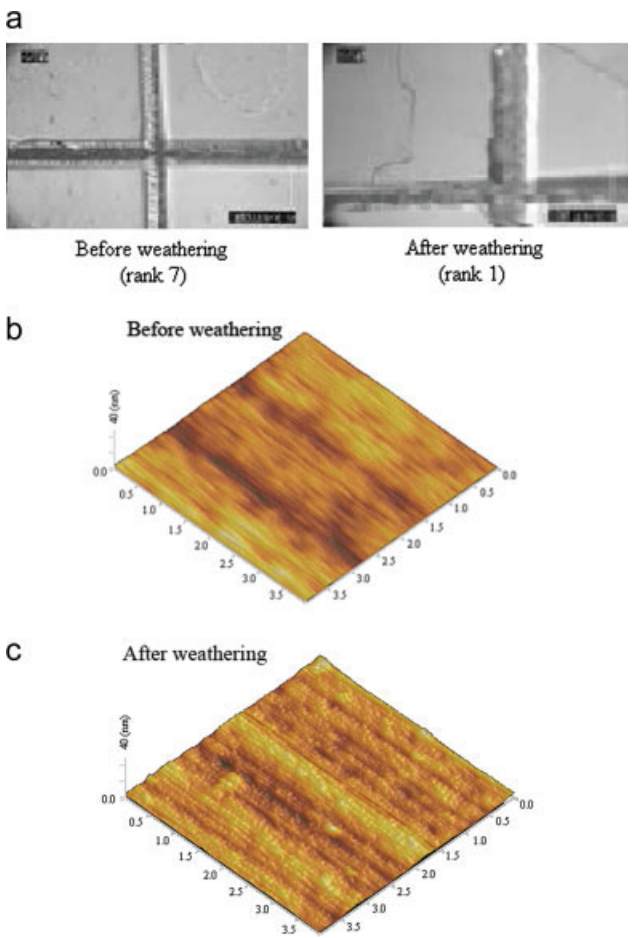

Figure 4 (a) The optical micrographs, (b) the AFM image of hybrid coating film before weathering, and (c) the AFM image of hybrid coating film after weathering. [Color figure can be viewed in the online issue, which is available at www.interscience.wiley.com.]

and also to initiate a radical polymerization under UV radiation.[32,33] Therefore, the postpolymerization may be likely to occur if the photoinitiator remains in the coating film. This continued postpolymerization could lead to shrinkage of the hybrid film due to the increase in crosslinking density. As a result, the surface roughness increases. FTIR spectroscopy investigation provides a further confirmation of such shrinkage. It showed the peak of Si—O—Si stretching band at 1024 cm^{-1} slightly shifted to higher wave number (1036 cm^{-1}) after weathering, assuming the contraction of Si—O—Si bond. The shrinkage of the film due to the contraction of Si—O—Si bond could induce strain at the interface.

It may be thought that the increase of strain could lead to a failure of the hybrid film at interface, the situation here may be different. In general, there are three possible modes of coating failure: (1) the interface failure due to poor adhesion or weakening of adhesion, (2) the coating layer failure due to the degradation or weakening of hybrid resin, and (3) failure at the substrate itself. A schematic representation of the possible degradation and failure process is depicted in Figure 5.

To understand which mode is most likely responsible for the adhesion failure, a detailed XPS investigation was conducted. The hybrid film before weathering could not be characterized by XPS analysis because it is difficult to remove the film from the substrate due to the excellent adhesion. However, the peeling of the film was completed at the interface of the substrate and the film after weathering. The hybrid film (after weathering) was removed from the substrate, and both sides of hybrid film and PTU substrate were subsequently evaluated by XPS analysis. The thickness of the deterioration layer detached from the substrate was estimated as $\sim$ 0.5 nm by XPS depth profile analysis of coating film side. The low resolution XPS survey scans (Figures are not shown) show no peak difference between bare substrate and the substrate after weathering. Silicon peak was not observed on the substrate survey scan, which is attributed from the crosslinked polymer, suggesting that the failure is not at the silsesquioxane hybrid coating layer side. However, the nitrogen and sulfur peaks in the hybrid film after weathering were observed and the existence of nitrogen and sulfur peaks on the hybrid film surface indicated the degradation of the substrate during weathering. It is clear that the effect of weathering is twofold: first, it leads to photodegradation of PTU as discussed later and weakens the substrate, and second, it also leads to a postpolymerization, which results in shrinkage of the coating layer. Because of the shrinkage, strain was exerted on the weakened PTU substrate, which leads to failure of the PTU substrate.

The atomic compositions of PTU substrates and hybrid films near the delaminated side before and after weathering are summarized in Table IV. The results show that nitrogen (N) and sulfur (S) elements attributed from thiourethane bond were found

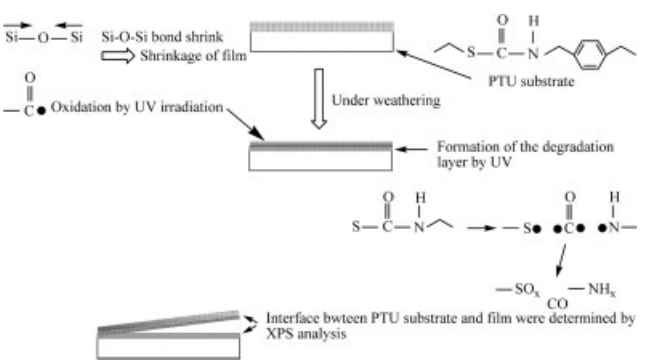

Figure 5 The schematic representation of the possible failure mechanism between the hybrid coating film and the PTU substrate.

TABLE IV
The Atomic Compositions of PTU Substrates and Hybrid Films Near the Exfoliation Side Before and After Weathering

		Atomic composition (wt %)				
		C	O	N	S	Si
PTU substrate	Bare substrate	69.7	10.3	7.1	12.9	–
	Substrate after weathering	61.8	18.8	7.1	12.3	–
Coating film	Initial film*	54.9	34.2	–	–	10.2
	Film after weathering	67.3	23.1	2.7	4.0	2.9

* Initial film means the film before weathering, coated on the polymer substrate to compare with the film after weathering.

in the after weathering film. The existence of N and S in the delaminated film suggests the deterioration of PTU substrate under UV radiation. In the next section, we will report on how to improve the weathering stability of hybrid coating by adding UV absorbers.

Figure 6 shows the high resolution of N 1s and S 2p core-level spectra taken over the bare substrate, the delaminated surfaces of the substrate, and the hybrid film sides after weathering in the presence of water. One component peak (399.7 eV) in N 1s signal was observed in the bare substrate, as seen in Figure 6(a), which is attributed to the thiourethane bond.[34] The binding energy of thiourethane bond slightly shifted to higher energy side (+0.2 eV) in the delaminated substrate (399.9 eV) but also reduced the component intensity of thiourethane peak, in comparison to the bare substrate. It appears that a substantial proportion of the thiourethane bond dissociated due to the strong penetration of the UV radiation into the PTU substrate. The formation of a new component peak at 401.8 eV was observed in both the delaminated surfaces of the substrate and the hybrid film sides after weathering. This may be ascribed to $—NH_x$ group formed by the dissociation of thiourethane bond as shown in Figure 5. It is assumed that the formation of amino bond leads to the high shift of binding energy of N 1s due to the decrease of electron density in N atom. Figure 6(b) displays that the S 2p signal is composed of two

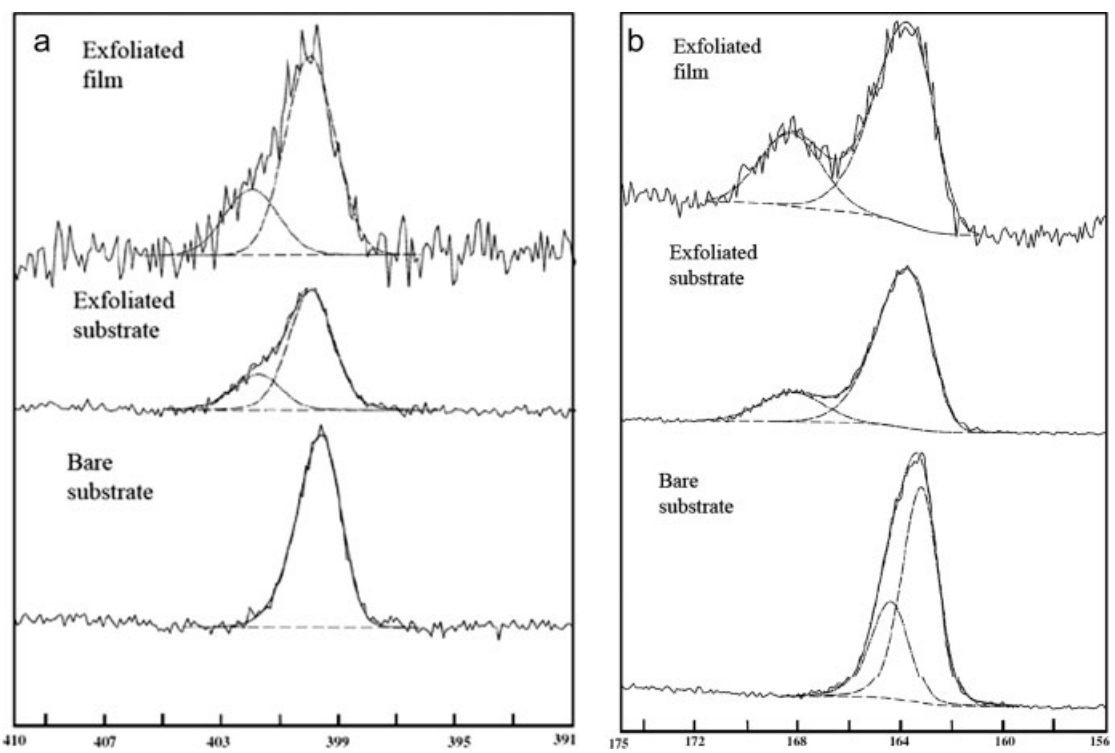

Figure 6 High resolution XPS spectra for the failure surface of the bare substrate, exfoliated surfaces of the substrate, and the hybrid film sides after weathering in the presence of water; (a) N 1s core-level spectra and (b) S 2p core-level spectra.

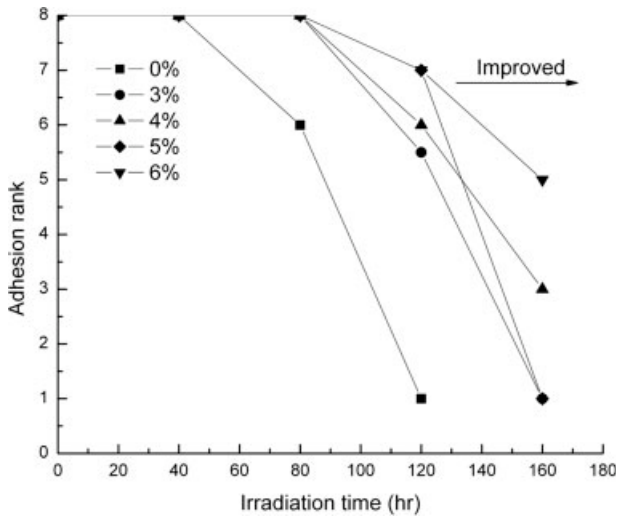

Figure 7 Adhesion versus UV irradiation time at various concentrations of UV absorbers.

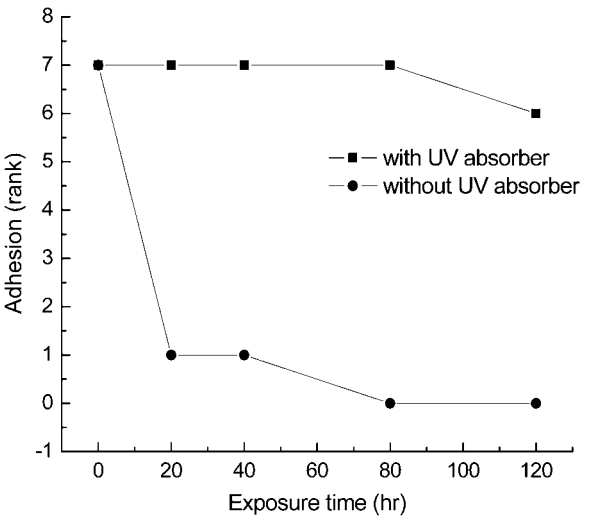

Figure 8 Adhesion versus UV radiation exposure time of hybrid coating films with and without UV absorbers. Adhesion was determined after weathering test for both hybrid coating films.

component peaks at 163.3 and 164.5 eV, which correspond to S $2p_{3/2}$ and S $2p_{1/2}$, respectively.[34] Interestingly, the two separated peaks were observed in the substrate and the hybrid film surfaces after weathering. The peaks represented at 163.8 eV in both sides attributed to the thiourethane bond. The new peaks appeared at high-energy side (168.3 eV) referred to the formation of $—SO_x$ group,[34] suggesting that it may occur from the fragmentation of thiourethane bond.

Effect of UV absorbers

It has been known that the weather resistance of hybrid coating materials can be greatly improved by the addition of UV absorbers in the resin formulation.[27–29] The key role of UV absorbers is to screen the UV light and prevent the UV radiation from penetrating into the polymer substrate to avoid the photodegradation of the substrate. In this study, various types of UV absorbers were examined and it appeared that a mixture of three different types of UV absorbers: 2,2′,4,4′-tetrahydroxybenzophenone (THBP), hydroxyphenyltriazine (HPT), and benzotriazole (BTZ) is most effective. The amount of UV absorbers added to the hybrid coating solution was optimized by UV spectroscopy (Figure is not shown). Figure 7 shows the adhesion versus irradiation time at various concentrations of added UV absorbers. It shows the excellent weather resistance under UV radiation during the short exposure time, but it deteriorated after longer irradiation time. The higher the concentration of UV absorber, the better resistance was observed.

Figure 8 shows the effect of UV absorbers on weather resistance of hybrid film on the PTU substrate. Weather resistance of the hybrid film without UV absorbers dramatically decreased under UV irradiation due to the postpolymerization and photodegradation occurring at the polymer substrate. For a sample with the addition of UV absorbers, almost no change in weather resistance was observed after 5 days of UV irradiation. This explains that UV absorbers protected the polymer substrate from the photodegradation and substantially improved the weather resistance of hybrid coating.

In this study, the amount of epoxy-functionalized CSSQ (OB-CSSQ) was optimized in the hybrid coating formulation. When a large amount of OB-CSSQ was added (>20 wt %) to the coating solution, the transparent coating film was not observed. It is speculated that OB-CSSQ segregated from the composition, and the hydrophobic group of CSSQ may aggregate on the surface of the hybrid coating as shown in Figure 9. The segregation has two parts: one is silicon's movement to surface, which was determined by XPS depth profile analysis; but this will not lead to nontransparency. The important segregation is phase separation which result in big domain size that scatter light.[35] The presence of the cage structure of silsesquioxane could be reduced

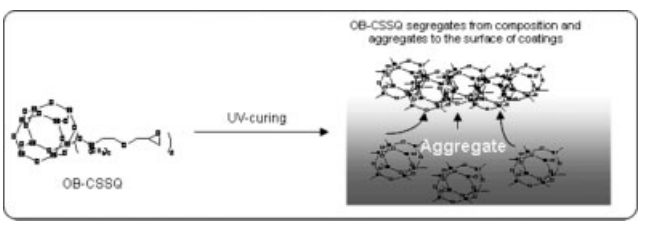

Figure 9 The schematic representation of OB-CSSQ aggregates in the hybrid coating film.

the detrimental effect of residual photoinitiator for postpolymerization.

CONCLUSIONS

New photocurable epoxy/cubic silsesquioxane hybrid materials are reported, and the failure of UV-curable hybrid coating on polythiourethane (PTU) substrate under weathering was studied using AFM, FTIR, and XPS analyses. It has found that the failure of adhesion is due neither to the degradation of cubic silsesquioxane nor to the failure of adhesion at interface. The degradation is due mainly to the PTU substrate which underwent photodegradation when subjected to UV and water condition. The increase of strain owing to the shrinkage of coating layer under UV radiation also contributes to the failure of the weakened PTU substrate. The weathering resistance of PTU substrate was significantly improved by applying cationic UV-curable hybrid coating with UV absorbers, which effectively protect the PTU substrate against weathering. The advantages of this hybrid coating include fast cure speed, solvent-free formulation, and improved mechanical and surface properties using epoxy-functionalized CSSQ.

References

1. Pappas, S. P. UV Curing Science and Technology; Plenum: New York, 1992; p 2.
2. Decker, C. Macromol Rapid Commun 2002, 23, 1067.
3. Takimoto, Y.; Fouassier, J. P.; Rabek, J. C. Radiation Curing in Polymer Science and Technology; Elsevier: London, 1993; Vol. III, p 269.
4. Sangermano, M.; Epicoco, E. P.; Priola, A.; Rizza, G.; Malucelli, G. Macromol Mater Eng 2007, 292, 634.
5. Mehnert, R.; Pincus, A.; Janorsky, I.; Stowe. R.; Berejka, A. In Wiley/Sita Series in Surface Coatings Technology; Wiley: New York, 1998; Vol. I, Chapter VIII.
6. Bajpai, M.; Shukla, V.; Habib, F. Prog Org Coat 2005, 53, 239.
7. Bulut, U.; Crivello, J. V. Macromolecules 2005, 38, 3584.
8. Crivello, J. V. J Polym Sci Part A: Polym Chem 2006, 44, 3036.
9. Crivello, J. V.; Mao, Z. Chem Mater 1997, 9, 1554.
10. Soh, M. S.; Yap, A. U. J.; Sellinger, A. Eur Polym J 2007, 43, 315.
11. Nebioglu, A.; Teng, G.; Soucek, M. D. J Appl Polym Sci 2006, 99, 115.
12. Ruiter, B.; El-ghayoury, A.; Hofmeier, H.; Schuber, U. S.; Manea, M. Prog Org Coat 2006, 55, 154.
13. Ji, W. G.; Hu, J. M; Liu, L.; Zhang, J. Q.; Cao, C. N. Prog Org Coat 2006, 57, 439.
14. Zhou, S.; Wu, L.; Sun, J. Prog Org Coat 2002, 45, 33.
15. Hajji, P.; David, L.; Gerard, J. F.; Pascault, J. P.; Vigier, G. J Polym Sci Part B: Polym Phys 1999, 37, 3172.
16. Gunji, T.; Iizuka, Y.; Arimitsu, K.; Abe, Y. J Polym Sci Part A: Polym Chem 2004, 42, 3676.
17. Su, H. W.; Chen, W. C.; Lee, W. C.; King, J. S. Macro Mater Eng 2007, 292, 666.
18. Lichtenhan, J. D.; Schwab, J. J., Sr.; Reinerth, W. A. Chem Innovat 2001, 1, 3.
19. Cheng, H.; Tamaki, R.; Laine, R. M.; Babonneau, F.; Chujo, Y.; Treadwell, D. R. J Am Chem Soc 2000, 122, 10063.
20. Zhang, C.; Laine, R. M. J Am Chem Soc 2000, 122, 6979.
21. Lamm, M. H.; Chen, T.; Glotzer, S. C. Nano Lett 2003, 3, 989.
22. Laine, R. M.; Choi, J.; Lee, I. Adv Mater 2001, 13, 800.
23. Choi, J.; Haecup, J.; Yee, A. F.; Zhu, Q.; Laine, R. M. J Am Chem Soc 2001, 123, 11420.
24. Li, G. Z.; Wang, L.; Tohiani, H.; Daulton, T. L.; Koyama, K., Jr.; Pittman, C. U. Macromolecules 2001, 34, 8686.
25. Feher, F. J.; Budzichowski, T. A. J Organomet Chem 1989, 379, 33.
26. Fong, H.; Dickens, S. H.; Flaim, G. M. Dent Mater 2005, 21, 520.
27. Decker, C.; Biry, S.; Zahouily, K. Polym Degrad Stab 1995, 49, 111.
28. Decker, C.; Biry, S. Prog Org Coat 1996, 29, 81.
29. Decker, C.; Zahouily, K. J Polym Sci Part A: Polym Chem 1998, 36, 2571.
30. Sellinger, A.; Laine, R. M. Chem Mater 1996, 8, 1592.
31. Mya, K. Y.; He, C.; Huang, J.; Xiao, Y.; Dai, J.; Siow, Y. P. J Polym Sci Part A: Polym Chem 2004, 42, 3490.
32. Decker, C.; Nguyen, T. V. T.; Decher, D.; Weber, K. E. Polymer 2001, 42, 5531.
33. Lingzhi, Z.; Zhigang, C.; Qingshui, Y.; Zhaoxi, L. J Appl Polym Sci 1999, 71, 1081.
34. Beamson, G.; Beiggs, D. High Resolution XPS of Organic Polymers: The Scienta ESCA300 Database; Wiley: England, 1992.
35. Huang, J.; He, C.; Liu, X.; Xu, J.; Tay, S. S.; Chow, S. Y. Polymer 2005, 46, 7018.